Title Page:

Full article title: Mild inflammation in healthy males induces fatigue mediated by changes in effective connectivity within the insula

Full names of all authors, in order, and their affiliations:

Kristian Stefanov [a], John McLean [b], Alison McColl [a], Neil Basu [a], Jonathan Cavanagh [a, c], and Rajeev Krishnadas [c]

a: Institute of Infection, Immunity & Inflammation, University of Glasgow, Glasgow G12 8QQ, Great Britain and Northern Ireland

b: Institute of Neurological sciences, Queen Elizabeth hospital, Glasgow, G51 4TF

c: Institute of Neuroscience & Psychology, University of Glasgow, Glasgow G12 8QQ, Great Britain and Northern Ireland

Short/running title: Allostatic model of the insula

Corresponding authors:

Rajeev Krishnadas; Institute of Neuroscience and Psychology, University of Glasgow, Room 638, 62 Hillhead Street, Glasgow, G12 8QB, Phone : 00441415313207; Rajeev.Krishnadas@glasgow.ac.uk

Kristian Stefanov: Imaging Centre of Excellence, Langlands Drive, Glasgow G51 4LB;

0044 1415416859; Kristian.Stefanov@glasgow.ac.uk

Abstract

Background:

Systemic inflammation is associated with sickness behaviors such as low mood and fatigue. Activity patterns within the insula are suggested to coordinate these behaviors but have not been modeled. We hypothesized that mild systemic inflammation would result in changes in effective connectivity between the viscerosensory and the visceromotor regions of the insula.

Methods:

We used a double-blind, crossover design to randomize 20 male subjects to receive either a *Salmonella typhi* vaccine or a placebo saline injection at two separate sessions. All participants underwent a resting-state functional magnetic resonance scan 3 hours after injection. We determined behavioral and inflammatory changes, using the Profile of Mood States questionnaire and interleukin-6 levels. We extracted effective connectivity matrices between bilateral mid/posterior (viscerosensory) and anterior (visceromotor) insular cortices using spectral dynamic causal modeling. We applied parametric empirical Bayes and mediation analysis to determine a vaccination effect on effective connectivity and whether this mediated behavioral changes.

Results:

The vaccine condition was associated with greater interleukin-6 levels and greater fatigue 3 hours after the injection. Activity within the right mid/posterior insula increased the activity within the bilateral anterior insular regions. This connectivity was augmented by vaccination over a 99% posterior confidence threshold. The right mid/posterior insula-to-left anterior insula connectivity was significantly associated with fatigue and mediated the association between inflammation and increased fatigue scores.

Conclusions:

These results demonstrate that increased effective connectivity between specific nodes of the insula can model and mediate the association between inflammation and fatigue in males.

ClinicalTrials.gov; NCT02653235. Trial Name: Impact of Immune Challenge on Triple Network Connectivity in Humans. https://clinicaltrials.gov/ct2/show/study/NCT02653235

Keywords: Allostasis, Dynamic causal models, Inflammation, Insula, Interoception, Sickness behavior

Introduction

Systemic inflammation is often associated with low mood, reduced appetite, poor concentration, psychomotor retardation, and fatigue, collectively called sickness behavior (1). Lipopolysaccharide and *Salmonella typhi* vaccine–induced increase in proinflammatory cytokines (e.g., interleukin [IL]-6) in humans is associated with sickness behavior, and animal knockout models of IL-6 are less sensitive to the behavioral aspects of lipopolysaccharide; both of these observations support a causal role for inflammation in the genesis of this phenotype (2-4). Neuroimaging studies using these experimental paradigms have shown differential activation of several brain regions that correlate with sickness behavior. For example, Harrison et al. (5, 6) demonstrated that typhoid vaccination–associated changes in the subgenual anterior cingulate cortex, brainstem hub, and medial temporal and posterior insular activity correlated with symptoms suggestive of human sickness. Similarly, Eisenberger et al. (7) found lipopolysaccharide-associated neural correlates of social disconnection and anhedonia. However, to better understand the genesis of these symptoms, it is essential to undertake a principled approach that examines the hierarchy under which the brain regions that process these inflammatory signals operate.

In keeping with this, Critchley and Harrison (8) brought together evidence to illustrate neuronal pathways that link peripheral interoceptive signals to the various regions of the brain. Briefly, immune cells activated by pathogen-associated molecular patterns release inflammatory mediators such as cytokines. These cytokines activate visceral afferents along the vagus nerve and the sensory circumventricular organs (9), whose signals are integrated within the thalamus and brainstem viscerosensory hubs, such as the periaqueductal gray and parabrachial nuclei. The information from these structures is then relayed to the mid/posterior insular cortex that primarily represents visceral input. Craig (10) suggested that the primary vagal A-delta and C fiber interoceptive signals are first represented in the posterior insula and then hierarchically integrated and abstracted

in the more anterior parts. The activity within the insula is, therefore, crucial in evoking visceral reflexes that result in a series of sickness behaviors (6).

The insula is structurally and functionally heterogeneous, lies deep within the lateral sulcus, and is divided by the central sulcus into an anterior part and a mid/posterior part. Studies using tract tracing, electrocortical stimulation, and functional imaging (11, 12) suggest a grossly posteroanterior anatomical and functional dichotomy, with the mid/posterior (granular) part involved in somato/viscerosensory mapping and the anterior (agranular) part involved in visceromotor, socioemotional, and cognitive control (13). More recently, the Embodied Predictive Interoception Coding model provides an integrated framework to explore the origins of sickness behavior within an anatomical, physiological, and computational hierarchy (14). It suggests that the anterior insular cortex (AIC) acts as a visceromotor cortex (VMC) to create "predictions" of expected visceral signals from previous experience. The VMC sends these predictions to the mid/posterior insula—the viscerosensory cortex (VSC) (**Figure 1**). The VMC also estimates the balance between the predicted requirements and the available inflammatory resources (e.g., cytokines) of the body. Based on this estimation, the VMC sends out motor signals to the hypothalamus, brainstem, and spinal cord to maintain homeostasis. In contrast, the VSC computes the difference between VMC predictions and thalamic interoceptive input based on Bayesian active inferences (15). This prediction error signal is transmitted back to the VMC to allow modification of its predictions or its motor signals.

In health, the VMC is relatively insensitive to small fluctuations (prediction error) in available inflammatory resources. This results in relatively stable predictions, manifested in undisrupted homeostasis. This stability of the VMC was evidenced by study from Simmons et al. (16) in which VMC activity was sensitive to food-specific images but was not modulated by levels of peripheral glucose, which was instead observed in the VSC.

An induced state of inflammation with greater fluctuations of cytokines (larger prediction errors) may disrupt this stability. This inflammatory demand would result in allostasis, a physiological and/or behavioral response to maintain functioning rather than sustain a narrow homeostatic range (17). In this context, how the mid-insular cortex (MIC) and AIC influence each other's activity might be a model of allostasis and sickness behavior genesis. In this study, we used the *S. typhi* vaccination model and IL-6 levels, as a measure of inflammation, during which we could study activity within different parts of the insula.

Based on the above framework, we hypothesized that 1) inducing systemic inflammation (typhoid vaccination–induced increase in IL-6) would cause changes in directed/effective connectivity [using dynamic causal modeling (18)] between the viscerosensory (mid/posterior) and visceromotor (anterior) insula; 2) connectivity would be increased from the mid/posterior insula to the AIC in the vaccination session compared with the placebo session, as a representation of an increased prediction error; and 3) these connectivity changes would mediate increased sickness behavior in vaccination.

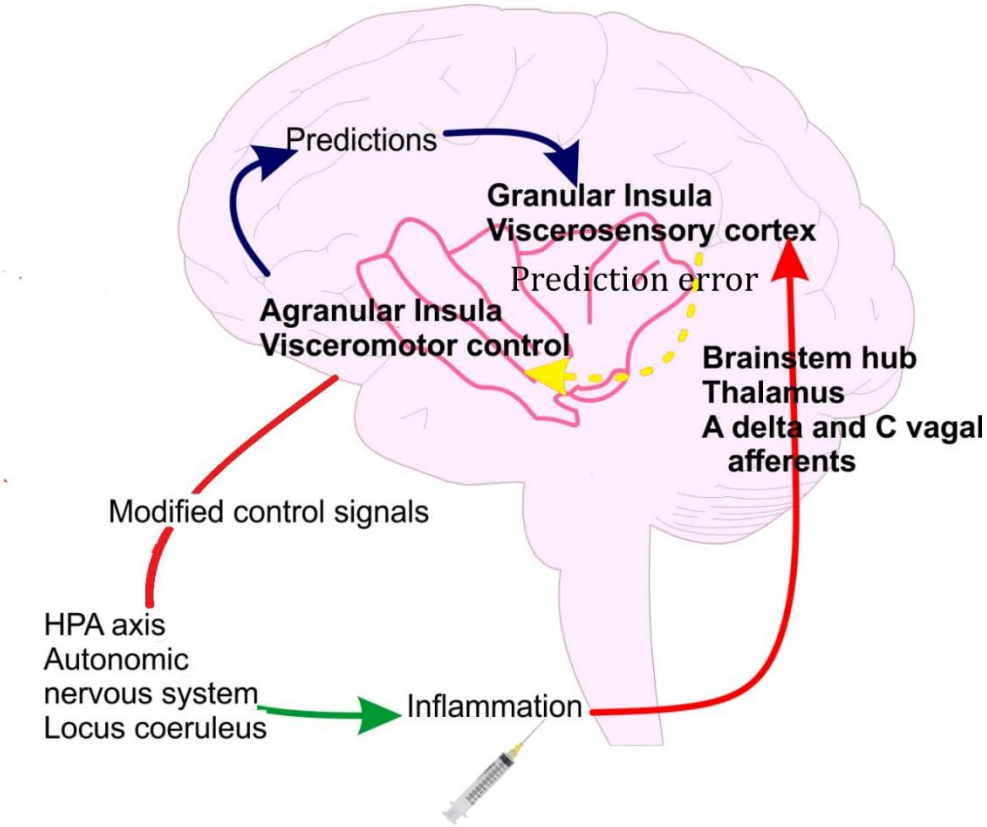

Figure 1: The insula within the Embodied Predictive Interoception Coding model (14). In health, the viscerosensory cortex, represented by the granular or mid/posterior insula, registers viscerosensory signals via the brainstem hub, thalamus, and A-delta and C vagal afferents. These signals would not differentiate extensively from the predictions sent from visceromotor regions represented by the agranular or anterior insula. Consequently, this would minimize the mismatch or prediction error sent back to the visceromotor regions. However, in inflammation, this circuit would cause large prediction errors, leading to the visceromotor regions sending control signals via the hypothalamic-pituitary-adrenal (HPA) axis, autonomic nervous system, and locus coeruleus in an attempt to reduce the prediction errors.

Methods and Materials

Participants and Design:

Ethics approval was obtained from the NHS Regional Ethics Committee, and all subjects provided informed consent. We utilized a randomized double-blind crossover trial design (**Figure 2**) with 2 conditions—*S. typhi* (typhoid) vaccine or placebo saline injection (6–8 weeks apart) (NCT02653235). The experimental design allowed us to explore causal mechanisms that link peripheral inflammation to brain connectivity. Twenty healthy males 20 to 50 years of age were recruited via the Glasgow University repository of potential participants. We excluded those with a history of medical and/or DSM-IV Axis I psychiatric condition; those who had a *S. typhi* vaccination over the last 3 years or any other vaccinations over the last 6 months; those who had taken antibiotics or anti-inflammatory agents (including nonsteroidal anti-inflammatory drugs) over the 2 weeks leading to the study; and those with a contraindication for *S. typhi* vaccination or magnetic resonance imaging (MRI). Participants were advised to not consume caffeinated beverages or alcohols, to avoid high-fat meals, to refrain from smoking on the day, and to refrain from excessive exercise for 12 hours before testing.

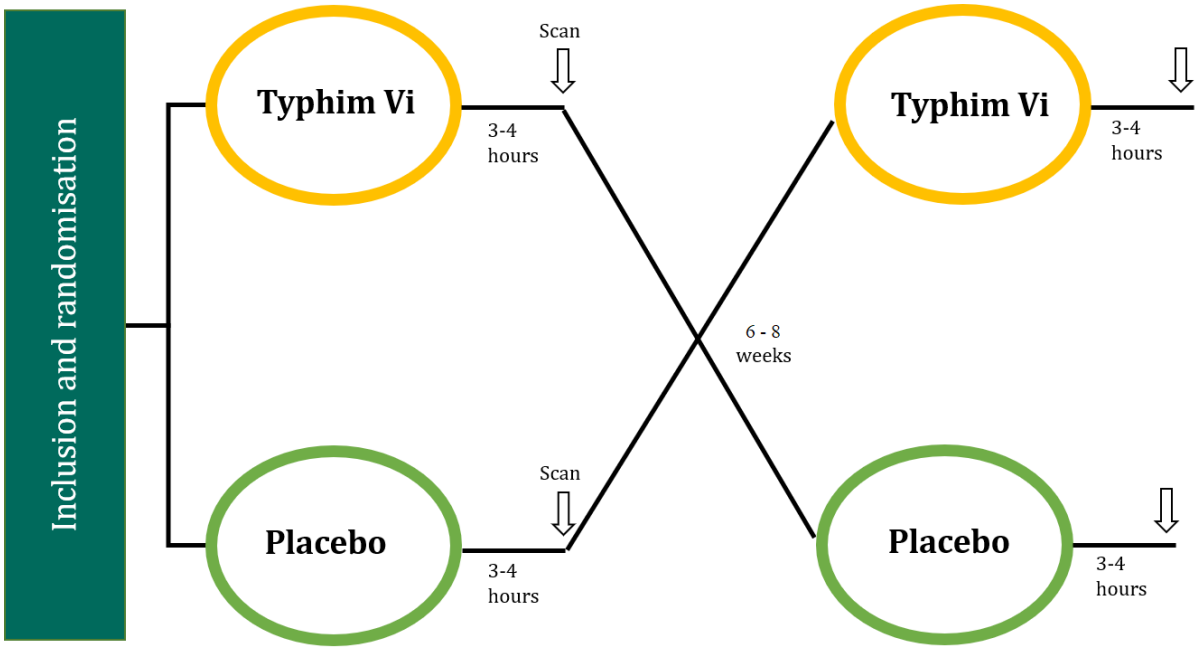

Figure 2: Experimental design. Twenty healthy male subjects were recruited and randomly allocated to receive either saline solution placebo or *Salmonella typhi* vaccine. After 6–8 weeks, the participants received the other injection. Plasma interleukin-6 and the Profile of Mood States behavioral questionnaire were taken prior to and 3–4 hours after injection, with a resting-state functional and structural magnetic resonance imaging scan at 3 hours postinjection.

Randomization and study procedure:

Briefly, at the first visit, participants were randomly assigned to receive either the vaccine or placebo at the initial visit, using a 1:1 allocation as per a randomization schedule generated and kept within the pharmacy. Allocation concealment was ensured, as the randomization code was not released until the analysis was completed. To ensure masking, the syringes were prefilled, and the injections were administered by a nurse independent of the study. The investigators and the participants were masked to the condition throughout the study, and the code for allocation was broken only at the end of the study. The injection was administered on the same arm on both occasions. All participants were first seen at 9 AM, when baseline measures and fasting cytokine levels were obtained. Following this, they were administered the placebo/vaccine. All participants were then scanned at around 3 hours after the injection. The 3-hour blood sample was collected soon after the scan.

The vaccine:

S. typhi (Typhim Vi) vaccine consisted of the Vi capsular polysaccharide typhoid vaccine (Sanofi Pasteur Europe, Lyon, France), 50-mg/mL virulence polysaccharide antigen of formaldehyde-inactivated *S. typhi*. The typhoid vaccine was selected as a low-grade stimulus to induce proinflammatory cytokine levels, comparable to patients with depression, and produce neural activation and behavioral components of sickness behavior, without any effect on joint pain, body temperature, or hemodynamics (5). The placebo was 0.5 mL of normal saline.

Clinical and IL-6 measurement:

All participants were screened using the Structured Clinical Interview for DSM-IV (19). Patients also completed the Profile of Mood States (POMS) (20), sensitive to sickness-like behaviors, at baseline and 3 hours postinjection. Body temperature and blood pressure were assessed at baseline and 3 hours after the injection. IL-6 levels were measured in plasma samples extracted before and 3 hours after the injection of vaccine or placebo. A sample of 10 mL of venous blood was drawn into BD Vacutainers (BD Biosciences, Franklin Lakes, NJ) containing K2EDTA and centrifuged immediately at 8000 rpm for 10 minutes. Plasma was collected and frozen at -80°C. IL-6 was measured in duplicate using Human IL-6 Quantikine High-Sensitivity ELISA kits (R&D Systems, Minneapolis, MN) as per the manufacturer's instruction. Optical densities were read using an Infinite 200 PRO TECAN microplate reader (Tecan, Männedorf, Switzerland) and were converted into concentrations against a 7-point standard curve. The kit sensitivity was 0.11 pg/mL and the intra- and interassay coefficients of variation were 10% and 11%, respectively.

MRI acquisition and pre-processing:

All scans were done 3 hours after receiving the vaccine/placebo. All images were acquired on a 3T GE Signa Excite HD system (GE Healthcare, Milwaukee, WI) with a 32-channel head coil. A structural T1 scan (repetition time = 2300 ms, echo time = 2.96 ms, 192 sagittal slices, 1-mm^3 isotropic voxels, and image resolution 256 x 256) was obtained for coregistration purposes. A resting-state functional MRI scan (10 minutes) was acquired. Participants were instructed to view a fixation cross while letting their mind wander. Resting-state data were collected with single-shot full k-space echo-planar imaging with ramp sampling correction using the intercommissural line (anterior commissure-posterior commissure) as a reference (repetition time = 2000 ms, echo time = 29 ms, matrix size = 64 x 64, 32 slices, voxel size = 3 x 3 x 4 mm^3, axial plane–series ascending–multislice mode; interleaved; 300 volumes).

Preprocessing was carried out using SPM12 (Wellcome Department of Cognitive Neurology, London, United Kingdom) and DPARSF (Data Processing Assistant for Resting-State fMRI version 4.4 (http://rfmri.org/DPABICamp4), both under the MATLAB platform (version 2018b) (The MathWorks, Inc., Natick, MA). Briefly, this included removal of first 5 volumes, head-movement correction, manual reorientation, T1 coregistration to functional scans, segmentation and normalization by DARTEL, and spatial smoothing (6-mm full width at half maximum). Six motion parameters, along with signals from the white matter [0 -24 -33] and cerebrospinal fluid [0 -40 -5], were used as confounds and regressed when specifying the general linear model for each subject and session (21). Additionally, a high-pass filter of 128-second cutoff was implemented.

Effective connectivity and analysis:

Based on a literature review on allostasis (22), Montreal Neurological Institute coordinates of bilateral AIC and MIC nodes focusing on interoception were chosen (**Table 1**), and individual time series were extracted from 8-mm spheres centered at the coordinates. The coordinates aligned with insula labels from a standard atlas of the SPM Anatomy toolbox (version 1.5) (23). To extract effective connectivity between and within these nodes, spectral dynamic causal modeling (DCM) was implemented. This is a method of inferring influences between regions that are directional and causal (24). It specifies a network model and generates cross-spectral densities based on that model. Parameters are estimated by inverting the model and take the form of effective connectivity matrices (25). Here, a fully connected DCM was specified and inverted for each subject and session. The DCM included 12 connections among the 4 insular regions and 4 self-connections. All DCMs were graphically represented to check for any subject or session with poorly explained variance (<10%) (26), with no DCM reaching that criterion and with a group mean of 93.84%. Effective connectivity matrices from these DCMs were then subjected to paired-samples nonparametric Wilcoxon signed-rank tests (W). Furthermore, parametric empirical Bayes (PEB) of the individual subjects' DCM parameters was specified and used

to model how the effects as part of a specified group confined connectivity parameters on each scanning session. This approach was used because of the added benefit over paired-samples tests of incorporating the variance of the connection strengths (27). The PEB design matrix had the commonalities (average) as the first covariate and session (placebo or vaccine) as the second covariate. Two additional PEBs were created for separate group DCM files of the placebo and vaccine sessions to construct representative matrices for each session. All three PEBs underwent Bayesian model reduction, in which all possible combinations of switching off connections (setting them at 0) were tested (27). This was performed to deduce whether the connections contributed to the model evidence (posterior probability [Pp]) relative to the covariates in the design matrix. The output was a Bayesian model average (BMA)—group-level connection strengths with the highest Pp—calculated by averaging across the reduced models within the fully connected PEB.

All statistical analyses were performed using JASP version 0.11.1 (28). The IL-6 values were negatively skewed and hence were log-transformed. We performed a repeated-measures analysis of variance test on the log-transformed IL-6 values to examine the group x time interaction. POMS scores were negatively skewed, and transformations did not render them normal. Therefore, we used a 2-tailed Wilcoxon signed-rank test (nonparametric) to examine the between-group difference in POMS scores at baseline and 3 hours postinjection. We used Spearman's correlation test to examine the relationship between effective connectivity strength and 3-hour postinjection fatigue scores (corrected for baseline fatigue). We used 2-tailed nonparametric Wilcoxon signed-rank tests to examine the between-group differences in effective connectivity between different nodes. We conducted an indirect-effects analysis to explore the relationship among condition (vaccine/placebo) (independent variable), effective connectivity (mediating/indirect variable), and 3-hour postvaccine POMS fatigue scores (dependent variable). The analysis here tests the hypothesis that the group membership (vaccination/placebo) accounts for some variance in the effective connectivity, and in

turn, this variance in effective connectivity accounts for a proportion of the variance in POMS scores. A bootstrap method was used to estimate the indirect effect and bias-corrected 95% confidence interval (CI) based on 10,000 bootstrap samples. This analysis requires no assumption regarding the underlying distributions because the statistical significance level is determined nonparametrically.

Table 1: Montreal Neurological Institute Coordinates of Volumes of Interest Selected for Effective Connectivity Analysis

Region	x	y	z	Reference
rAIC	38	20	-2	(29)
lAIC	-34	20	-2	(29)
lMIC	-38	-2	-1	(30)
rMIC	48	5	-6	(31)

lAIC, left anterior insular cortex; lMIC, left middle insular cortex; rAIC, right anterior insular cortex; rMIC, right middle insular cortex.

Results

One participant dropped out and another had excess movement in the scanner. Therefore, we analyzed data from 18 subjects. The mean age of the sample was 25.63 ± 6.51 years, with a mean body mass index of 22.76 ± 2.17 kg/m^2. Neither placebo nor vaccination was associated with a significant change in body temperature ($p > .05$) or systolic/diastolic blood pressure ($p > .05$). None of the participants exhibited any injection-site discomfort, pain, or swelling at 3 hours.

The vaccine condition was associated with increase in inflammatory markers

Using a repeated-measures analysis of variance, we found that there was a significant effect of group ($F_{1,17} = 33.69$, $p < .001$) and time ($F_{1,17} = 24.31$, $p < .001$), and a group x time interaction ($F_{1,17} = 35.99$, $p < .001$), on IL-6 levels (**Figure 3**).

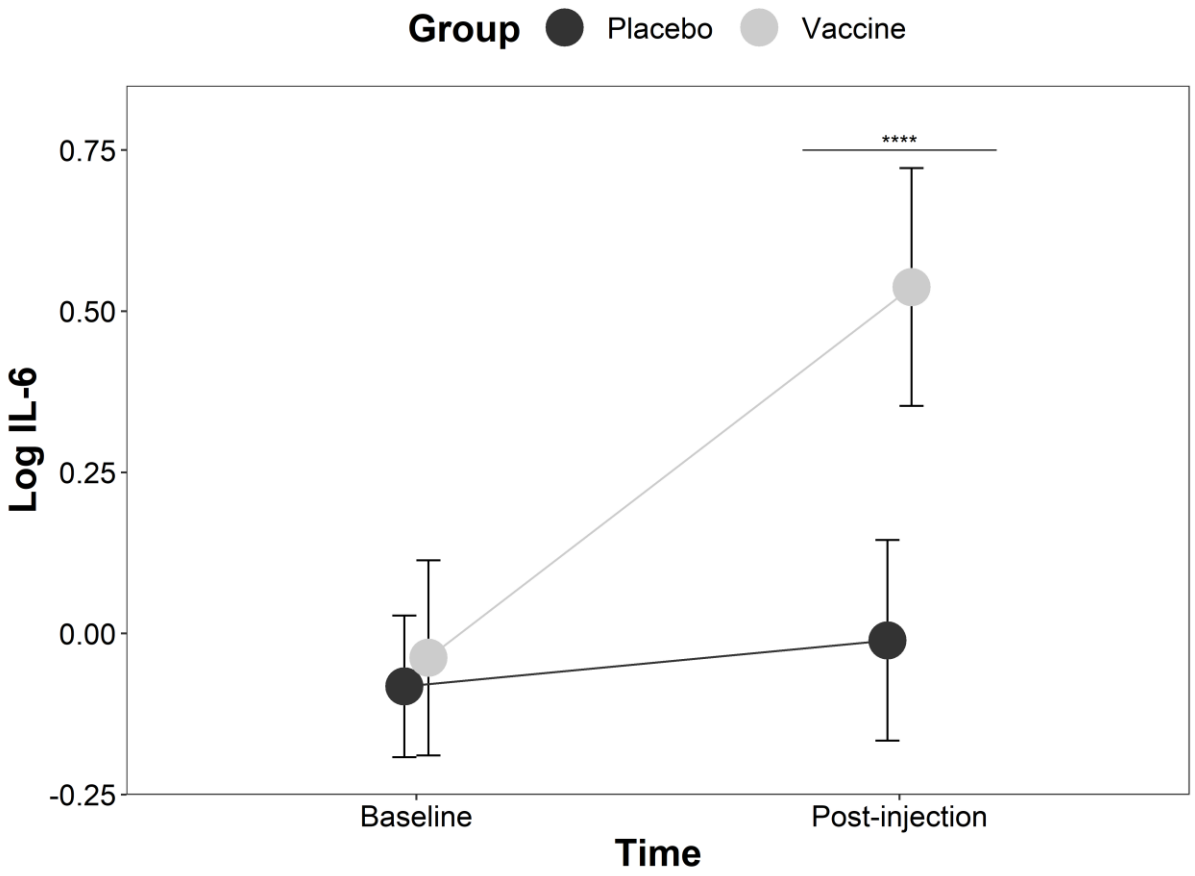

Figure 3: Plot of interleukin (IL)-6 levels (log-transformed) as measured by enzyme-linked immunosorbent assay at baseline and 3 hours after injection. There was a significant difference at the $p < .001$ level between the placebo and vaccine conditions based on a repeated-measures analysis of variance (error bars depict 95% confidence intervals of the mean). ****$p < .001$

The vaccine condition was associated with greater fatigue at 3 hours compared with the placebo condition

There were no between-group differences in any POMS scores at baseline. The vaccine condition was associated with greater fatigue scores at 3 hours (W = 43.5, p = .01) than the placebo condition. There were no other between-group differences in the 3-hour POMS scores (**Figure 4**).

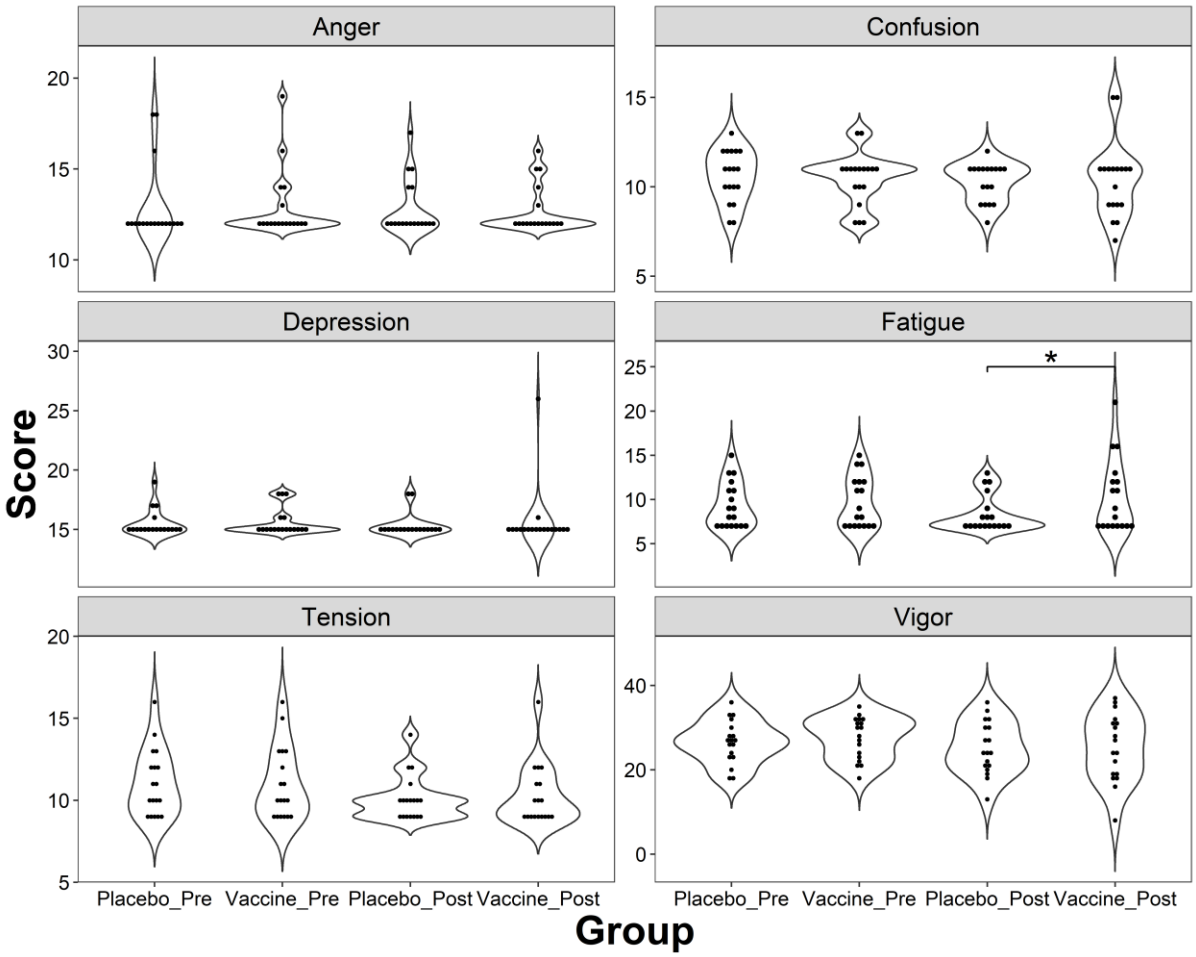

Figure 4: Violin plots of mean Profile of Mood States subscores at baseline and 3 hours postinjection are shown for both the vaccine and placebo conditions. *p < .05.

The vaccine condition was associated with greater effective connectivity between the MIC and AIC

For illustrative purposes, the positioning of the 4 volumes of interest, as well as the representative matrices for placebo and vaccine from the separate BMAs, are shown in **Figure 5**.

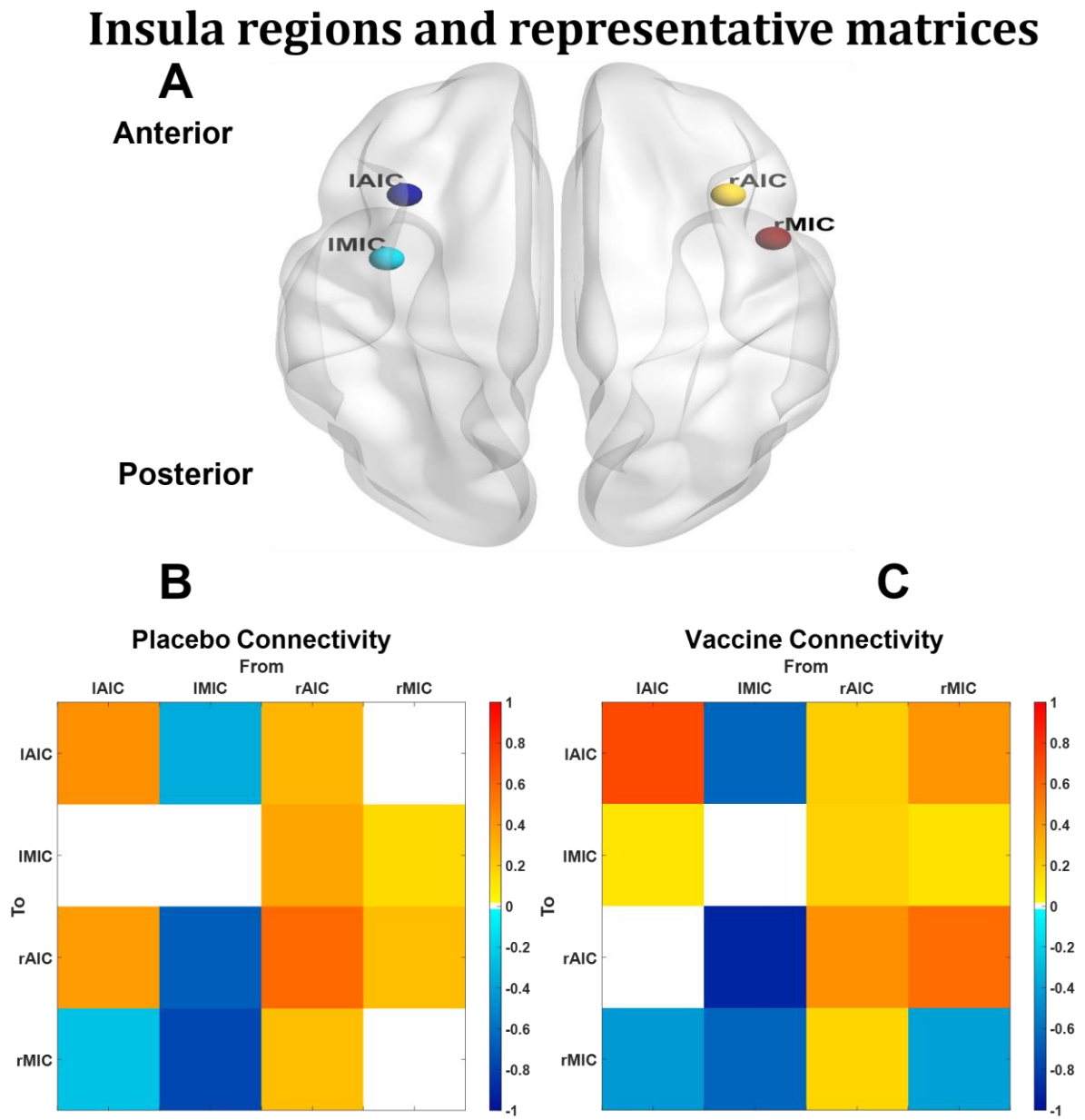

Figure 5: Illustrative images of the 4 insula volumes of interest and the average effective connectivity matrices of the placebo and vaccination sessions. **(A)** The nodes of the 4 volumes of interest (coordinates from **Table 1**) are imposed on a smoothed Montreal Neurological Institute template using BrainNet Viewer software (32). The mean effective connectivity matrices, in units of Hz, extracted from the Bayesian model average of the separate Bayesian general linear models (parametric empirical Bayes) for the **(B)** placebo and **(C)** vaccination sessions. The matrices were set above a free energy threshold of 99% posterior probability, with white squares representing the connections that did not survive the threshold. lAIC, left anterior insular cortex; lMIC, left middle insular cortex; rAIC, right anterior insular cortex; rMIC, right middle insular cortex.

Difference in effective connectivity: The effective connectivity parameters between the right MIC (rMIC) and the left MIC (W = 148, p = .04 [false discovery rate corrected], rankbiserial correlation [r_{rb}] = 0.731 [95% CI, 0.384–0.897]) and right AIC (rAIC) (W = 157, p

= .0144 [false discovery rate corrected], r_{rb} = 0.836 [95% CI, 0.593–0.94]) were significantly higher in the vaccination session compared with the placebo session.

PEB – session difference: **Figure 6** shows group-level effective connectivity parameters relative only to vaccination in the described insular network. Identical to the nonparametric tests, the rMIC → left AIC (lAIC) and rMIC → rAIC are the only two connectivity parameters that survived a nonzero criterion with a Pp of 99% using a free energy threshold.

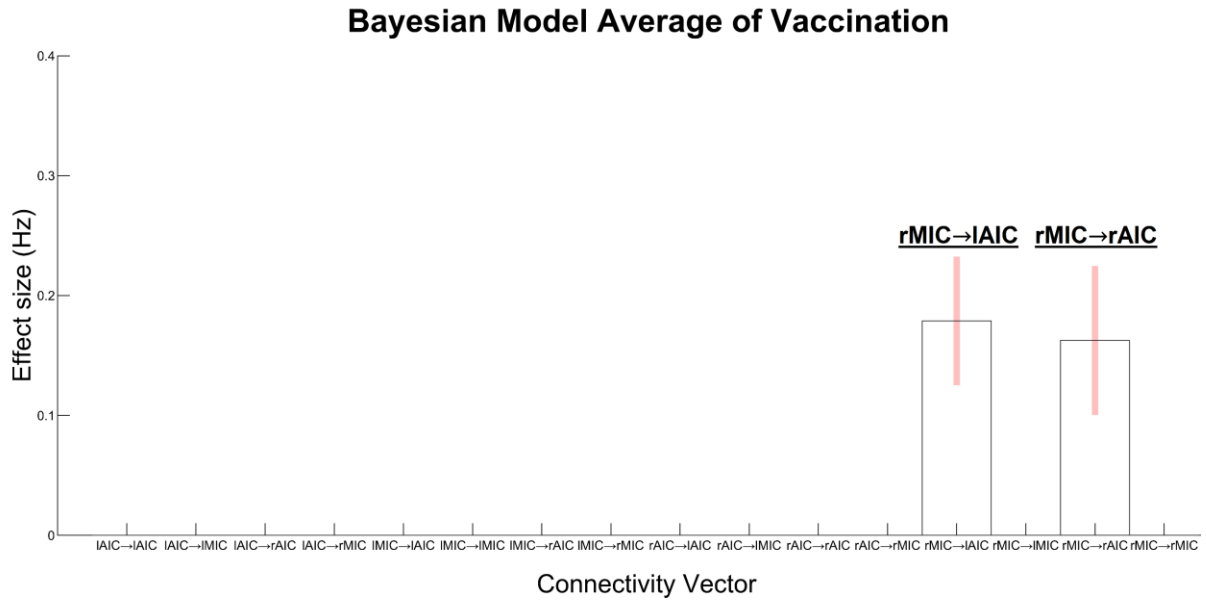

Figure 6: Greater effective connectivity between right mid-insular cortex (rMIC) and left and right anterior insular cortex (lAIC and rAIC) in vaccination. The format of X → Y represents a vector in which X affects (symbolized by →) the activity of Y. The figure shows a Bayesian model average of posterior empirical Bayes parameter estimates relative to vaccination, over a threshold of 99% posterior probability (very strong effect). The variance (uncertainty) is shown as pink bars. The bar heights depict a 0.179-Hz increase of excitatory rMIC → lAIC (average = 0.305 Hz) and 0.163-Hz increase of excitatory rMIC → rAIC (average = 0.405 Hz) by vaccination (n = 18). lMIC, left mid-insular cortex.

Effective connectivity mediated the association between the vaccine condition and POMS scores

Because 3-hour fatigue scores were greater in the vaccine condition, we explored whether effective connectivity from the rMIC to rAIC/lAIC mediated the above relationship (**Figure 7**). Greater effective connectivity of the rMIC → lAIC was associated with greater fatigue scores (r = .35, p = .03). Greater effective connectivity between the rMIC → rAIC was

associated with greater fatigue scores but did not reach statistical significance (r = .2, p = .2). We found a statistically significant indirect effect of effective connectivity between the rMIC → lAIC on fatigue scores (indirect effect = 0.16, SE = 0.116 [95% CI, 0.01–0.50]; r^2 = .06 [95% CI, .001–.17]), which explained about 6% of the variance in the fatigue scores explained by vaccination.

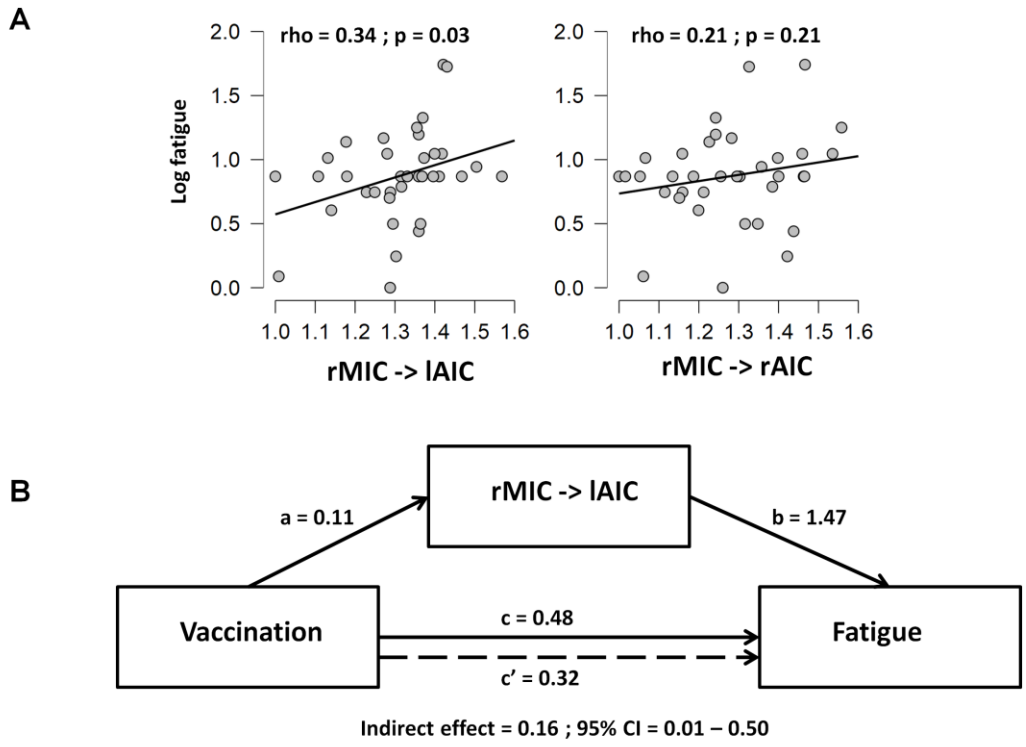

Figure 7: Depiction of how insula connectivity associates with fatigue, and whether it mediates it as a result of vaccination. **(A)** Spearman's correlation between effective connectivity and log transformed fatigue scores, corrected for baseline fatigue. Only the right mid-insular cortex (rMIC) → left anterior insular cortex (lAIC) was found to be significant. **(B)** The relationship among vaccination status, effective connectivity strength, and fatigue scores. The mediation analysis partitions the total variance (total effect [c]) explained by the predictor into a part that is independent of the mediating variable (direct effect [c']), and a part that is accounted for via the mediating variable (indirect effect). The indirect effect is essentially the product of coefficients of a' and b' paths. Baseline fatigue score was included as a covariate in the model. CI, confidence interval; rAIC, right anterior insular cortex.

Discussion

Using a double-blind, placebo-controlled design, we have shown that inducing a mild inflammatory stimulus via typhoid vaccine in healthy males was associated with greater effective connectivity from the right mid/posterior insula (VSC) to the bilateral AIC (VMC). This, in turn, was associated with greater levels of fatigue. Adding to previous research on the inflammation-brain-behavior axis (5, 33, 34), this study's use of effective connectivity described a likely hierarchy of how inflammation-associated brain regions interact in mediating a behavioral change. Essentially, the data suggest that inflammation-induced visceral information flows from viscerosensory to visceromotor insular regions, induces symptoms suggestive of fatigue, and is initiated mostly from the right hemisphere.

The right laterality, observed in this study, is consistent with findings from previous visceral sensation and stimulation studies (35-38), which demonstrate an association between right insular cortex activity and interoceptive bodily states, represented by autonomic homeostatic afferents. There is some evidence to suggest that responses to increased systemic inflammation originate from the sympathetic nervous system (39). Further evidence for laterality stems from studies that show an association between the right dorsal AIC activity and salience mapping, and lAIC and reward-related behavior (40, 41). Finally, interhemispheric communication between the right and left insulas is thought to occur through structural fibers along the midbody of the corpus callosum (42).

Our finding of greater posterior-to-anterior connectivity possibly represents the flow of visceral signals through an anteroposterior microscopic gradient of the insula, in which the posterior region has a classic 6-layer structure (granular), whereas the anterior region lacks a granular layer 4 (agranular). Within the Embodied Predictive Interoception Coding model framework (14), agranular regions would react on received feedback from granular regions only when the expected (predictions) and actual sensory inputs are substantially different (large prediction errors), for instance, in an induced inflammatory state as in our

study. Consequently, as these feedback connections were the only significant contrasts between the placebo and vaccine conditions in participants, we propose that the increase in effective connectivity in the bilateral AIC was due to ascending signals that possibly coded for prediction errors. However, to confirm these signals as prediction errors, the cortical layers of both their origin within the MIC and their target in the AIC need to be elucidated by techniques such as laminar functional MRI (43). The Embodied Predictive Interoception Coding model (14) also implies that the diminished reactivity of agranular regions in health is due to a reduction in the influence of prediction errors by neuromodulatory neurons (dopaminergic, cholinergic) and GABAergic (gamma aminobutyric acidergic) interneurons within the upper layers of the granular regions. Such may be the case during inflammation, which is known to affect these neuromodulatory systems (44). In the context of this study, the precision weighting of prediction errors may be more prominent in interoception because of a lower signal-to-noise ratio of visceral signals (45). Inflammation may, therefore, alter this precision weighting, leading to greater prediction errors in the form of stronger granular (posterior) to agranular (anterior) connectivity.

We observed an increase in fatigue scores, similar to other inflammation induction and observational studies (46). In this context, computational theories of allostatic control suggest that core symptoms of sickness behavior such as fatigue may be a metacognitive evaluation of failed homeostatic control—in our case, inflammatory response to the vaccine (22). This inflammatory response can be considered as an interoceptive surprise: a mismatch between viscerosensory input (VSC) and the brain's generative model (from VMC) of this input. Ideally, this mismatch would trigger a homeostatic response that corrects the mismatch. However, the inability to correct for the large prediction errors can lead to a metacognitive response that represents the ongoing fruitless effort to regulate homeostasis (inflammation). We speculate that the association between the

greater effective connectivity among the primary VSC (MIC), the VMC (AIC), and fatigue is representative of such a metacognitive response.

Our study has several limitations. First, pain (nociceptive) effects from the vaccine could confound inferences about inflammation, as nociceptive lamina 1 pathways also relay in the interoceptive insula (47). However, participants did not exhibit any pain or swelling at the injection site at 3 hours postinjection. Second, our mediation analysis was probably underpowered, given the small sample size. Nevertheless, we argue that such an approach has added value to what is essentially an experimental design. The mediation explained only around 6% of the variance in the total effect, an effect that was yet robust enough to be detected using the small number of subjects (48). It is possible that the correlation between fatigue and rMIC → rAIC connectivity strength was not significant, owing to a lack of power (49). Last, although we described a likely hierarchy of how the VSC and VMC interact, a more comprehensive body of work is required to establish it as a Bayesian inference model of interoceptive processing.

Ideally, conclusive work would model and manipulate both the timing and connectivity of predictions, prediction errors, and their precision weighting. In future studies, this could be done through laminar functional MRI and simultaneous electroencephalography recordings, using advanced techniques that can incorporate layer-specific information, while separating vascular and neural components of the blood oxygen level–dependent signal (50-52). To manipulate the prediction coding parameters, future work would also require experimental paradigms that utilize interoceptive perturbation techniques [for a review, see (53)] such as manipulation of breathing load (54) and enable construction of models to infer the parameters' trajectories in a subject-specific manner. For example, Harrison et al. (55) measured prediction errors for motivational behavior through such a task, in which participants learned how to gain monetary rewards and avoid losses. In the context of interoception, precision weighting can be altered by shifting attention (56) and/or the statistical structure of stimulus sequences (57).

In the future, Bayesian inference models can help improve psychiatric and psychosomatic diagnoses. Current nosological systems group together people with heterogeneous symptoms and possibly different pathological mechanisms (58), and thus are not informative enough to predict clinical or treatment outcomes at an individual basis (59). Using Bayesian models can address these weaknesses because they incur mechanistic insight by depicting the location and process being disrupted in disease-relevant circuits. For example, exploring the relationship among inflammation, brain, and sickness behavior, within the context of interoception, there are 5 hierarchical levels that could be investigated, over a hierarchy that Stephan et al. (22) have already described: 1) sensory inputs from the periphery, 2) perceptions (inferences in viscerosensory areas), 3) forecasting (predictions constructed by visceromotor areas), 4) actions (e.g., homeostatic motor signals from visceromotor areas to effector regions), and 5) metacognition.

Theoretically, disruptions at any of the above levels can be operationalized as a failure of signaling and/or computation of predictions, prediction errors, and their precision. Such knowledge could then direct pharmacological strategies, as each of these quantities may be related to different classes of neurotransmitters (60). Additionally, there are a variety of clinical practices specific to targeting these computational quantities (61), such as increasing the precision of sensory input through mindfulness training (62). Targeting these parameters should be conjugated with findings of how modulatory neurons and glia affect interoception during inflammation (63). Ultimately, these interoceptive models would allow clinicians to predict and monitor patient-specific efficacy of psychological and pharmacological treatments of sickness-like behaviors in psychiatry.

Conclusion

We have shown that inducing mild inflammation through a typhoid vaccine can increase the influence of lower to higher interoceptive regions of the insula and mediate significantly higher fatigue as an exemplar of sickness-like behavior. If the current limits of investigating processing at the cortical layer level are overcome, interoceptive models can be the basis for describing and targeting the pathological mechanisms in psychiatric disorders.

Acknowledgements and Disclosures

This work was supported by an Academy of Medical Sciences Clinical Lecturer Starter Grant (to RK). We thank all the participants and the Glasgow Clinical Research facility and NHS Greater Glasgow and Clyde pharmacy for helping conduct the study. We thank Becky Allan (medical student) for helping with data entry. The results of this study have been previously published in abstract form (64). The authors report no biomedical financial interests or potential conflicts of interest.

ClinicalTrials.gov; Impact of Immune Challenge on Triple Network Connectivity in Humans; https://clinicaltrials.gov/ct2/show/study/NCT02653235;

NCT02653235.

References

1. Dantzer R, O'Connor JC, Freund GG, Johnson RW, Kelley KW (2008): From inflammation to sickness and depression: when the immune system subjugates the brain. *Nature Reviews Neuroscience*. 9:46-57.
2. Shattuck EC, Muehlenbein MP (2016): Towards an integrative picture of human sickness behavior. *Brain Behavior and Immunity*. 57:255-262.
3. Hingorani AD, Cross J, Kharbanda RK, Mullen MJ, Bhagat K, Taylor M, et al. (2000): Acute systemic inflammation impairs endothelium-dependent dilatation in humans. *Circulation*. 102:994-999.
4. Bluthe RM, Michaud B, Poli V, Dantzer R (2000): Role of IL-6 in cytokine-induced sickness behavior: a study with IL-6 deficient mice. *Physiology & Behavior*. 70:367-373.
5. Harrison NA, Brydon L, Walker C, Gray MA, Steptoe A, Critchley HD (2009): Inflammation Causes Mood Changes Through Alterations in Subgenual Cingulate Activity and Mesolimbic Connectivity. *Biological Psychiatry*. 66:407-414.
6. Harrison NA, Brydon L, Walker C, Gray MA, Steptoe A, Dolan RJ, et al. (2009): Neural Origins of Human Sickness in Interoceptive Responses to Inflammation. *Biological Psychiatry*. 66:415-422.
7. Eisenberger NI, Berkman ET, Inagaki TK, Rameson LT, Mashal NM, Irwin MR (2010): Inflammation-Induced Anhedonia: Endotoxin Reduces Ventral Striatum Responses to Reward. *Biological Psychiatry*. 68:748-754.
8. Critchley HD, Harrison NA (2013): Visceral Influences on Brain and Behavior. *Neuron*. 77:624-638.
9. Steinberg BE, Silverman HA, Robbiati S, Gunasekaran MK, Tsaava T, Battinelli E, et al. (2016): Cytokine-specific Neurograms in the Sensory Vagus Nerve. *Bioelectronic medicine*. 3:7-17.
10. Craig AD (2002): How do you feel? Interoception: the sense of the physiological condition of the body. *Nature Reviews Neuroscience*. 3:655-666.
11. Kurth F, Zilles K, Fox PT, Laird AR, Eickhoff SB (2010): A link between the systems: functional differentiation and integration within the human insula revealed by meta-analysis. *Brain Structure & Function*. 214:519-534.
12. Stephani C, Vaca GF-B, Maciunas R, Koubeissi M, Lueders HO (2011): Functional neuroanatomy of the insular lobe. *Brain Structure & Function*. 216:137-149.
13. Uddin LQ, Nomi JS, Hebert-Seropian B, Ghaziri J, Boucher O (2017): Structure and Function of the Human Insula. *Journal of Clinical Neurophysiology*. 34:300-306.
14. Barrett LF, Simmons WK (2015): Interoceptive predictions in the brain. *Nature Reviews Neuroscience*. 16:419-429.
15. Paulus MP, Feinstein JS, Khalsa SS (2019): An Active Inference Approach to Interoceptive Psychopathology. *Annual Review of Clinical Psychology, Vol 15*. 15:97-122.
16. Simmons WK, Rapuano KM, Kallman SJ, Ingeholm JE, Miller B, Gotts SJ, et al. (2013): Category-specific integration of homeostatic signals in caudal but not rostral human insula. *Nature Neuroscience*. 16:1551-1552.
17. Sterling P (2014): Homeostasis vs Allostasis Implications for Brain Function and Mental Disorders. *Jama Psychiatry*. 71:1192-1193.

18. Friston KJ, Preller KH, Mathys C, Cagnan H, Heinzle J, Razi A, et al. (2017): Dynamic causal modelling revisited. *NeuroImage*.
19. (1994): *Diagnostic and statistical manual of mental disorders : DSM-IV*. Fourth edition. Washington, DC : American Psychiatric Association, [1994] ©1994.
20. McNair DM (1984): CITATION CLASSIC - MANUAL FOR THE PROFILE OF MOOD STATES. *Current Contents/Social & Behavioral Sciences*.20-20.
21. Ashburner J, Barnes G, Chen C, Daunizeau J, Flandin G, Friston K, et al. (2016): SPM12 manual.
22. Stephan KE, Manjaly ZM, Mathys CD, Weber LAE, Paliwal S, Gard T, et al. (2016): Allostatic Self-efficacy: A Metacognitive Theory of Dyshomeostasis-Induced Fatigue and Depression. *Frontiers in Human Neuroscience*. 10.
23. Eickhoff S (2016): SPM Anatomy toolbox.
24. Razi A, Kahan J, Rees G, Friston KJ (2015): Construct validation of a DCM for resting state fMRI. *Neuroimage*. 106:1-14.
25. Kahan J, Foltynie T (2013): Understanding DCM: Ten simple rules for the clinician. *Neuroimage*. 83:542-549.
26. Zeidman P, Jafarian A, Corbin N, Seghier ML, Razi A, Price CJ, et al. (2019): A tutorial on group effective connectivity analysis, part 1: first level analysis with DCM for fMRI. *arXiv preprint arXiv:190210597*.
27. Friston KJ, Litvak V, Oswal A, Razi A, Stephan KE, van Wijk BCM, et al. (2016): Bayesian model reduction and empirical Bayes for group (DCM) studies. *Neuroimage*. 128:413-431.
28. JASPTeam (2020): JASP (Version 0.12.2)[Computer software].
29. Gu X, Hof PR, Friston KJ, Fan J (2013): Anterior insular cortex and emotional awareness. *Journal of Comparative Neurology*. 521:3371-3388.
30. Avery JA, Drevets WC, Moseman SE, Bodurka J, Barcalow JC, Simmons WK (2014): Major Depressive Disorder Is Associated With Abnormal Interoceptive Activity and Functional Connectivity in the Insula. *Biological Psychiatry*. 76:258-266.
31. Simmons WK, Avery JA, Barcalow JC, Bodurka J, Drevets WC, Bellgowan P (2013): Keeping the Body in Mind: Insula Functional Organization and Functional Connectivity Integrate Interoceptive, Exteroceptive, and Emotional Awareness. *Human Brain Mapping*. 34:2944-2958.
32. Xia M, Wang J, He Y (2013): BrainNet Viewer: A Network Visualization Tool for Human Brain Connectomics. *Plos One*. 8.
33. Harrison NA, Cooper E, Dowell NG, Keramida G, Voon V, Critchley HD, et al. (2015): Quantitative Magnetization Transfer Imaging as a Biomarker for Effects of Systemic Inflammation on the Brain. *Biological Psychiatry*. 78:49-57.
34. Hannestad J, Subramanyam K, Della Gioia N, Planeta-Wilson B, Weinzimmer D, Pittman B, et al. (2012): Glucose Metabolism in the Insula and Cingulate Is Affected by Systemic Inflammation in Humans. *Journal of Nuclear Medicine*. 53:601-607.
35. Kuhtz-Buschbeck JP, van der Horst C, Wolff S, Filippow N, Nabavi A, Jansen O, et al. (2007): Activation of the supplementary motor area (SMA) during voluntary pelvic floor muscle contractions - An fMRI study. *Neuroimage*. 35:449-457.
36. Kuhtz-Buschbeck JP, van der Horst C, Pott C, Wolff S, Nabavi A, Jansen O, et al. (2005): Cortical representation of the urge to void: A functional magnetic resonance imaging study. *Journal of Urology*. 174:1477-1481.

37. Zaki J, Davis JI, Ochsner KN (2012): Overlapping activity in anterior insula during interoception and emotional experience. *Neuroimage*. 62:493-499.
38. Oppenheimer SM, Gelb A, Girvin JP, Hachinski VC (1992): CARDIOVASCULAR EFFECTS OF HUMAN INSULAR CORTEX STIMULATION. *Neurology*. 42:1727-1732.
39. Pongratz G, Straub RH (2014): The sympathetic nervous response in inflammation. *Arthritis Research & Therapy*. 16.
40. Kann S, Zhang S, Manza P, Leung H-C, Li C-SR (2016): Hemispheric Lateralization of Resting-State Functional Connectivity of the Anterior Insula: Association with Age, Gender, and a Novelty-Seeking Trait. *Brain Connectivity*. 6:724-734.
41. Menon V, Uddin LQ (2010): Saliency, switching, attention and control: a network model of insula function. *Brain Structure & Function*. 214:655-667.
42. van der Knaap LJ, van der Ham IJM (2011): How does the corpus callosum mediate interhemispheric transfer? A review. *Behavioural Brain Research*. 223:211-221.
43. Norris DG, Polimeni JR (2019): Laminar (f)MRI: A short history and future prospects. *Neuroimage*. 197:643-649.
44. Felger JC, Treadway MT (2017): Inflammation Effects on Motivation and Motor Activity: Role of Dopamine. *Neuropsychopharmacology*. 42:216-241.
45. Damasio A, Carvalho GB (2013): OPINION The nature of feelings: evolutionary and neurobiological origins. *Nature Reviews Neuroscience*. 14:143-152.
46. Hanken K, Eling P, Hildebrandt H (2014): The representation of inflammatory signals in the brain - a model for subjective fatigue in multiple sclerosis. *Frontiers in Neurology*. 5.
47. Craig AD (2003): Pain mechanisms: Labeled lines versus convergence in central processing. *Annual Review of Neuroscience*. 26:1-30.
48. Friston KJ (2013): Sample size and the fallacies of classical inference. *Neuroimage*. 81:503-504.
49. Fritz MS, MacKinnon DP (2007): Required sample size to detect the mediated effect. *Psychological Science*. 18:233-239.
50. Scheeringa R, Koopmans PJ, van Mourik T, Jensen O, Norris DG (2016): The relationship between oscillatory EEG activity and the laminar-specific BOLD signal. *Proceedings of the National Academy of Sciences of the United States of America*. 113:6761-6766.
51. Markuerkiaga I, Barth M, Norris DG (2016): A cortical vascular model for examining the specificity of the laminar BOLD signal. *Neuroimage*. 132:491-498.
52. Heinzle J, Koopmans PJ, den Ouden HEM, Raman S, Stephan KE (2016): A hemodynamic model for layered BOLD signals. *Neuroimage*. 125:556-570.
53. Khalsa SS, Lapidus RC (2016): Can Interoception Improve the Pragmatic Search for Biomarkers in Psychiatry? *Frontiers in Psychiatry*. 7.
54. Paulus MP, Flagan T, Simmons AN, Gillis K, Kotturi S, Thom N, et al. (2012): Subjecting Elite Athletes to Inspiratory Breathing Load Reveals Behavioral and Neural Signatures of Optimal Performers in Extreme Environments. *Plos One*. 7.
55. Harrison NA, Voon V, Cercignani M, Cooper EA, Pessiglione M, Critchley HD (2016): A Neurocomputational Account of How Inflammation Enhances Sensitivity to Punishments Versus Rewards. *Biological Psychiatry*. 80:73-81.
56. Vossel S, Mathys C, Daunizeau J, Bauer M, Driver J, Friston KJ, et al. (2014): Spatial Attention, Precision, and Bayesian Inference: A Study of Saccadic Response Speed. *Cerebral Cortex*. 24:1436-1450.

57. Lecaignard F, Bertrand O, Gimenez G, Mattout J, Caclin A (2015): Implicit learning of predictable sound sequences modulates human brain responses at different levels of the auditory hierarchy. *Frontiers in Human Neuroscience*. 9.
58. Cuthbert BN, Insel TR (2013): Toward the future of psychiatric diagnosis: the seven pillars of RDoC. *Bmc Medicine*. 11.
59. Stephan KE, Bach DR, Fletcher PC, Flint J, Frank MJ, Friston KJ, et al. (2016): Charting the landscape of priority problems in psychiatry, part 1: classification and diagnosis. *Lancet Psychiatry*. 3:77-83.
60. Adams RA, Stephan KE, Brown HR, Frith CD, Friston KJ (2013): The computational anatomy of psychosis. *Frontiers in psychiatry*. 4:47-47.
61. Farb N, Daubenmier J, Price CJ, Gard T, Kerr C, Dunn BD, et al. (2015): Interoception, contemplative practice, and health. *Frontiers in Psychology*. 6.
62. Pagnoni G, Porro CA (2014): Cognitive modulation of pain and predictive coding Comment on "Facing the experience of pain: A neuropsychological perspective" by Fabbro and Crescentini. *Physics of Life Reviews*. 11:555-557.
63. Savitz J, Harrison NA (2018): Interoception and Inflammation in Psychiatric Disorders. *Biological psychiatry Cognitive neuroscience and neuroimaging*. 3:514-524.
64. Stefanov K, McLean J, Allan B, Basi N, Cavanagh J, Krishnadas R (2019): Abstract# 4295 Effective connectivity within the insula mediates the association between inflammation and human sickness behaviour. *Brain, Behavior, and Immunity*. 81:24.